



The Society shall not be responsible for statements or opinions advanced in papers or discussion at meetings of the Society or of its Divisions or Sections, or printed in its publications. Discussion is printed only if the paper is published in an ASME Journal. Authorization to photocopy for internal or personal use is granted to libraries and other users registered with the Copyright Clearance Center (CCC) provided \$3/article is paid to CCC, 222 Rosewood Dr., Danvers, MA 01923. Requests for special permission or bulk reproduction should be addressed to the ASME Technical Publishing Department.

Copyright © 1999 by ASME

All Rights Reserved

Printed in U.S.A.

DYNAMIC STABILITY IN A CRACKED TURBO BLADE-DISK

J. H. Kuang and B. W. Huang



Department of Mechanical Engineering
National Sun Yat-Sen University
Kaohsiung, TAIWAN, R. O. C.

(Phone:+886-7-525-2000 FAX:+886-7-5254299 E-Mail: kuang@mail.nsysu.edu.tw)

ABSTRACT

Analysis of the stability in a cracked blade-disk system is proposed. The effect of modal localization on the stability in a rotating blade-disk was studied. A crack near the root of a blade is regarded as a local disorder in this periodically coupled blade system. Hamilton's principle and Galerkin's method were used to formulate the equations of motion for the cracked blade-disk. The instability regions of this cracked blade-disk system were specified by employing the multiple scales perturbation method. Numerical results indicate that the rotation speed, shroud stiffness and crack depth in the blades affect the stability regions of this mistuned system significantly.

Keywords: stability, modal localization, crack, blade-disk

NOMENCLATURE

A = cross section area of the blade
 a = depth of crack
 b_0 = width at the root of the blade
 b_1 = width at the tip of the blade
 $c.c.$ = complex conjugate
 E = Young's modulus
 $f(t)$ = the variation of the rotation speed
 F_j = the magnitude of the perturbation speed
 F_M = the maximum of components of F_j
 k_s = shroud stiffness
 L = length of the blade
 N = total number of blades
 p^* = centrifugal force
 P_b = bending moment at crack
 $p_i^s(t), q_i^s(t)$ = determined coefficients

r_0 = position of the coupled shroud
 r^* = position of the crack
 R_h = root diameter of the turbo disk
 s = the number of blade
 t_0 = thickness at the root of blade
 t_1 = thickness at the tip of blade
 U_s^k = strain energy stored in the s^{th} shroud
 U_s^e, U_s^Ω = strain energy introduced by the bending moment and the centrifugal force
 u_s, v_s = deflections of the s^{th} blade
 u_ξ, v_ξ = deflections of the cracked blade
 ϵ = perturbation parameter
 $\phi_i^s(r)$ = comparison functions ($i=1,2,\dots$)
 λ_i = coefficients
 μ = Poisson's ratio
 θ = pretwisted angle of the blade
 ρ = density of the blade
 Ω = rotation speed of the disk
 Ω_0 = the steady speed
 ω = exciting frequency
 ω_j = perturbation frequency
 ω_0, ω_n = reference and natural frequencies

1. INTRODUCTION

Cracks frequently appear in rotating machinery due to manufacturing flaws or cyclic fatigue during operation. Especially in turbo-disks, numerous cracks can be observed after severe operating conditions [Bernstein and Alien (1992), Walls, deLaneville and Cunningham (1997)]. Local structural irregularity, some disorder, caused by cracks on the blade may change the dynamic behavior of a mistuned system

significantly. In a weakly coupled periodic structure with local structural or material irregularities, the modal localization phenomenon was investigated by Bendiksen (1987), Hodges (1982), Wei and Pierre (1988a, 1988b), Orgun and Tongue (1994), Kuang and Huang (1997). Such localization may in turn localize the vibration modes and thereby confine the vibration energy.

The shrouded bladed disk of a turbo-rotor can be regarded as a periodic system if all of the blades are assembled periodically. The dynamic behavior of such a shrouded blade-disk system has been studied by Cottney and Ewins (1974), whereas the fundamental aspects of dynamic response in mistuned turbo-machinery rotors have been studied by Afolabi (1985), Basu and Griffin (1985) and Kaneko et al (1994). For purposes of application, the design of turbo-machinery trends more and more towards high efficiency, so the complex shapes of blades in turbo-machinery is unavoidable. To consider the effect of the blade on the dynamic behaviors of a turbo-disk, periodically coupled taper beams are used herein to simulate the blades of a turbo-disk. For the sake of simplicity, the tapered pretwisted beams are approximated as Euler-Bernoulli beams. Similar models were proposed by Rao (1972a, 1977b). During actual service, the rotating speed of a shrouded blade-disk is subjected to a small range of variations under external disturbance. So, the parametric instability of a rotating blade-disk system with non-constant speed is worthy of study. Most of the studies on the stability are limited to the tuned systems, [Nayfeh et al. (1979), Hsu (1961), Young (1991), and Liao and Huang (1995)], where there is no local disorder. Only a few studies, such as Bendiksen (1984), on the dynamic stability in mistuned systems, have been conducted. Even if the stability regions exhibit similar sensitivity to disorder, Bendiksen (1984), few investigators turn their attention to this phenomenon, presumably because such consequences are believed to be always stabilizing.

The dynamic instability of a mistuned system should be worthy of attention because the structural or material irregularities in a turbo disk system are unavoidable. In this investigation, the dynamic instability in a shrouded pretwisted blade-disk with a cracked blade is studied. A time-varying rotational speed which is characterized as a small periodic perturbation superimposed on a steady state velocity is considered. The pretwisted Euler-Bernoulli beams are used to approximate the blades of a disk. The discrete modal localization equation of this mistuned system was derived by using the Galerkin method. The method of multiple scales was used to specify the regions of instability in this cracked blade-disk.

2. EQUATIONS OF MOTION

The periodic shrouded blade structure at a constant rotating speed Ω is shown in Fig. 1(a). It consists of a rigid hub with radius R_h and a cyclic assembly of N coupled blades. Each blade is coupled with the adjacent one through a shroud. The length of cantilever beam is L , and every blade is coupled by a shroud ring

to the adjacent one at position r_c . The individual blade modeled as the tapered pretwisted beam is displayed in Fig. 1(b). The thickness and breadth at the root of the blade are t_0 and b_0 . The transverse flexible deflections of the s th blade in the rotational plane and perpendicular to the rotational plane are denoted by components $v_s(r, t)$ and $u_s(r, t)$ respectively.

2.1 Blades without crack

Due to the bending vibration, the kinetic energy of the rotating s th taper blade can be displayed as

$$T_s = \frac{1}{2} \int_0^L \rho A \left\{ [\dot{u}_s(r, t)]^2 + [\dot{v}_s(r, t)]^2 + [\Omega v_s(r, t)]^2 \right\} dr \quad (1)$$

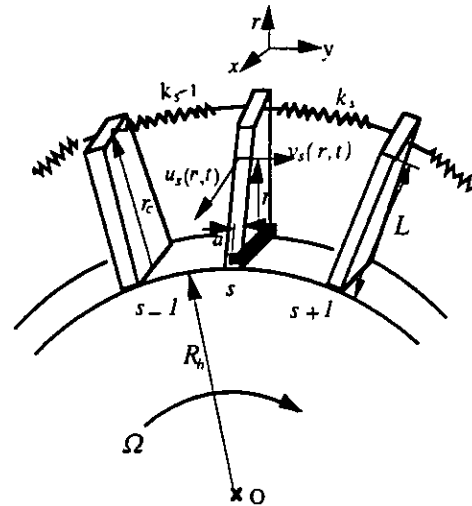
The cross sectional area of the taper beam at position r is

$$A(r) = b_0 t_0 \left(1 - \alpha \frac{r}{L} \right) \left(1 - \beta \frac{r}{L} \right) \quad (2)$$

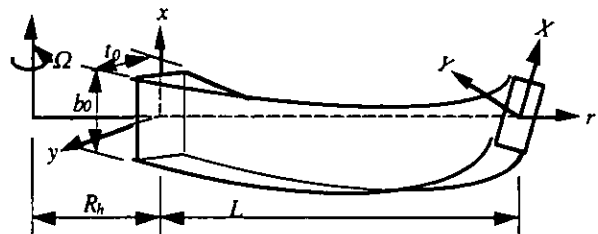
and

$$\alpha = \frac{b_0 - b_l}{b_0}; \quad \beta = \frac{t_0 - t_l}{t_0} \quad (3)$$

The total strain energy of the s th blade comprises three components



(a) Geometry of the blade-disk system



(b) Geometry of the pretwisted taper blade

Figure 1 Geometry of a rotating blade-disk

$$U_s = U_s^e + U_s^\Omega + U_s^k \quad (4)$$

where U_s^e , U_s^Ω and U_s^k are strain energy components introduced by the bending deformation, centrifugal force, and the elastic deformation of the shroud. They are

$$U_s^e = \frac{1}{2} \int_0^L E \left[I_{yy} (u_s'')^2 + 2I_{xy} (u_s'')(v_s'') + I_{xx} (v_s'')^2 \right] dr \quad (5)$$

$$U_s^\Omega = \frac{1}{2} \int_0^L p^* \left[(u_s')^2 + (v_s')^2 \right] dr \quad (6)$$

$$U_s^k = \frac{k_{s+1}}{2} \left[v_{s+1}(r_c, t) - v_s(r_c, t) \right]^2 \quad (7)$$

where $p^*(r)$ and k_{s+1} are the centrifugal force and the stiffness of the shroud ring. E is the Young's modulus of the blade and I_{xx} , I_{yy} and I_{xy} are the area moments in this article. Consider the disk blade, to be pretwisted with a uniform twist angle θ , and then the area moments at the position r can be derived as

$$I_{xx} = I_{XX} \cos^2\left(\frac{r}{L}\theta\right) + I_{YY} \sin^2\left(\frac{r}{L}\theta\right) \quad (8a)$$

$$I_{yy} = I_{XX} \sin^2\left(\frac{r}{L}\theta\right) + I_{YY} \cos^2\left(\frac{r}{L}\theta\right) \quad (8b)$$

$$I_{xy} = I_{XX} \sin^2\left(\frac{r}{L}\theta\right) + I_{YY} \cos^2\left(\frac{r}{L}\theta\right) \quad (8c)$$

where

$$I_{XX} = \frac{b_0 t_0^3}{12} \left(1 - \alpha \frac{r}{L}\right) \left(1 - \beta \frac{r}{L}\right)^3 \quad (9a)$$

$$I_{YY} = \frac{b_0^3 t_0}{12} \left(1 - \alpha \frac{r}{L}\right)^3 \left(1 - \beta \frac{r}{L}\right) \quad (9b)$$

For stability analysis, the rotational speed is considered to be not perfectly steady. A small perturbation speed, $f(t)$, is superimposed upon the steady state speed Ω_0 , i.e.,

$$\Omega = \Omega_0 + f(t) \quad (10)$$

If the speed Ω_0 is much smaller than the first natural frequency of the beam, the centrifugal force p^* may be approximated as a steady force [Anderson (1975), Young (1991)].

$$p^* = \int_r^L \rho A \Omega_0^2 (r + R_h) dr \quad (11)$$

So, using Hamilton's principle, the equation of motion of the s th blade, for time variable speed, can be expressed as

$$\rho A \ddot{u}_s - \rho \Omega_0^2 \left[\int_r^L A(r + R_h) dr u_s' \right] + E \left(I_{yy} u_s'' + I_{xy} v_s'' \right) = 0 \quad (12a)$$

$$\rho A \ddot{v}_s - \rho \Omega_0^2 \left\{ A v_s + \left[\int_r^L A(r + R_h) dr v_s' \right] \right\} + E \left(I_{xx} v_s'' + I_{xy} u_s'' \right) + (k_{s+1} + k_s) v_s \delta(r - r_c) - k_{s+1} v_{s+1} \delta(r - r_c) - k_s v_{s-1} \delta(r - r_c) = \rho A (2\Omega_0 f + f^2) v_s \quad (12b)$$

where $\delta(r - r_c)$ is the delta function. The boundary conditions are

$$u_s = v_s = u_s' = v_s' = 0, \quad \text{at } r = 0 \quad (13a)$$

$$u_s'' = v_s'' = u_s''' = v_s''' = 0, \quad \text{at } r = L \quad (13b)$$

The solutions for the above eigenvalue problem, i.e., Eqs (12a) and (12b), are assumed in the form

$$u_s(r, t) = \sum_{i=1}^m p_i^s(t) \phi_i^s(r) \quad v_s(r, t) = \sum_{i=1}^m q_i^s(t) \phi_i^s(r) \quad (14)$$

where $p_i^s(t)$ and $q_i^s(t)$ are coefficients to be determined and $\phi_i^s(r)$ are comparison functions. To simplify these notations, two nondimensional variables $\bar{r} = r/L$ and $\bar{r}_c = r_c/L$ are introduced. The exact bending modes of a pretwisted taper beam, as shown in Lee (1995), have been used to approximate the comparison functions in this study. Applying Galerkin's method, the equations of motion of the s th blade, i.e., Eqs 12(a) and (b), can then be approximated in the matrix form as

$$[m]_s \begin{Bmatrix} \ddot{p} \\ \ddot{q} \end{Bmatrix}_s + [k]_s \begin{Bmatrix} p \\ q \end{Bmatrix}_s - k_s \left[\Lambda^{s-1} \right] \begin{Bmatrix} p \\ q \end{Bmatrix}_{s-1} + (k_{s+1} + k_s) \left[\Lambda^s \right] \begin{Bmatrix} p \\ q \end{Bmatrix}_s - k_{s+1} \left[\Lambda^{s+1} \right] \begin{Bmatrix} p \\ q \end{Bmatrix}_{s+1} = (2\Omega_0 f + f^2) [d]_s \begin{Bmatrix} p \\ q \end{Bmatrix}_s \quad (15)$$

where the matrices are

$$[m]_s = \begin{bmatrix} [m]^{uu} & 0 \\ 0 & [m]^{vv} \end{bmatrix}_s; \quad [k]_s = \begin{bmatrix} [k^e]^{uu} + [k^\Omega]^{uu} & [k^e]^{uv} \\ [k^e]^{uv} & [k^e]^{vv} + [k^\Omega]^{vv} \end{bmatrix}$$

$$[d]_s = \begin{bmatrix} 0 & 0 \\ 0 & [d]^{vv} \end{bmatrix}_s \quad (16)$$

The disturbance component matrix $[d]^{vv}$ is identical to the component mass matrix $[m]^{vv}$. The matrices $[m]_s$, $[k]_s$ and $[d]_s$ are the mass, the stiffness and the perturbation matrix respectively, as shown in Kuang (1998). Then, the superscripts uu and vv denote components that are related to the rotational direction and the outoff plane direction. The superscripts uv denote components that are introduced from the coupling effect. For the stiffness, the superscripts e and Ω denote the stiffness which is related to the elastic deformation or the rotational speed respectively.

For convenience, the same comparison functions are employed for all of the blades without a crack. So, the matrices $[\Lambda^{s-1}]$, $[\Lambda^s]$ and $[\Lambda^{s+1}]$ for blades without a crack are identical.

They can be expressed as

$$[\Lambda^{s-1}] = [\Lambda^s] = [\Lambda^{s+1}] = [\Lambda] \quad (17)$$

$$[\Lambda] = \begin{bmatrix} 0 & 0 \\ 0 & \{\phi\}_s \{\phi\}_s^T \end{bmatrix}_{\bar{r}=\bar{r}_c} \quad (18)$$

with $\{\phi(\bar{r})\}_s = [\phi_1^s(\bar{r}), \phi_2^s(\bar{r}), \dots, \phi_m^s(\bar{r})]^T$

2.2 Blade with a crack

A number of papers [Rizos, Aspragathos and Dimarogonas (1990), Broke (1986), Tada *et al.* (1973)] have explored the effect of cracks on the dynamic and static behaviors of structures.

More recent articles by Chen *et al.* (1988) and Grabowski (1980) also dealt with the effects of cracks in rotating machinery. The cracked shrouded blade-disk may be regarded as a mistuned periodical system, if a crack is located at $\bar{r} = \bar{r}^*$ of the ξ th blade. Besides the strain energy caused by bending moment, rotating speed and shroud stiffness, the total strain energy of the defective blade will consist of the released energy caused by the cracks. They are

$$U_{\xi} = U_{\xi}^e + U_{\xi}^{\Omega} + U_{\xi}^k - U_{\xi}^c \quad (19)$$

where U_{ξ}^c is the released energy of a crack for the ξ blade. The mode 1 loading will be considered to dominate the stress field, when the crack is initiated by in plane bending fatigue. According to Dimarogonas's (1983) and Krawczuk's (1993) investigations, alteration of the elastic deformation energy in places on the crack caused by lateral bending moments are the only important changes in the case of slender beams. Therefore, the released energy of this crack may be approximated as

$$U_{\xi}^c = b_0(1 - \alpha \bar{r}^*) \int_0^a \frac{(1 - \mu^2)}{E} K_I^2 da \quad (20)$$

where a , μ are the depth of the crack and Poisson's ratio for the blade and K_I is the stress intensity factor under mode 1 loading. The stress intensity factor K_I can be estimated from the equation proposed by Tada *et al.* (1973).

$$K_I = \frac{6 p_b}{i_0^2 b_0 (1 - \alpha \bar{r}^*) (1 - \beta \bar{r}^*)^2} \sqrt{\pi \bar{y} i_0 (1 - \beta \bar{r}^*)} F_I(\bar{y}) \quad (21)$$

where the variables for a near root crack can be approximated as

$$p_b = EI_{xx} v_{\xi}'' \Big|_{\bar{r}=\bar{r}^*} \quad \text{and} \quad \bar{y} = \frac{a}{i_0(1 - \beta \bar{r}^*)} \quad (22)$$

$$F_I(\bar{y}) = \sqrt{\frac{2}{\pi \bar{y}} \tan\left(\frac{\pi \bar{y}}{2}\right)} \frac{0.923 + 0.199 \left[1 - \sin\left(\frac{\pi \bar{y}}{2}\right)\right]^4}{\cos\left(\frac{\pi \bar{y}}{2}\right)} \quad (23)$$

Adapting Eq. (20) gives

$$U_{\xi}^c = 3E(1 - \mu^2) i_0 (1 - \beta \bar{r}^*) \int_0^1 I_{xx} Q(\bar{y}) (v_{\xi}'')^2 \delta(\bar{r} - \bar{r}^*) d\bar{r} \quad (24)$$

where $\delta(\bar{r} - \bar{r}^*)$ is the delta function and

$$Q(\bar{y}) = \int_0^{\bar{r}} \pi \bar{y} F_I^2(\bar{y}) d\bar{y} \quad (25)$$

Similarly, the equation of motion for the ξ th cracked blade can be rewritten in the matrix form as follows,

$$\begin{aligned} [m]_{\xi} \begin{Bmatrix} \ddot{p} \\ \ddot{q} \end{Bmatrix}_{\xi} + [k]_{\xi} \begin{Bmatrix} p \\ q \end{Bmatrix}_{\xi} - k_{\xi} \begin{Bmatrix} \Lambda^{\xi-1} \\ \Lambda^{\xi-1} \end{Bmatrix} \begin{Bmatrix} p \\ q \end{Bmatrix}_{\xi-1} + (k_{\xi+1} + k_{\xi}) \begin{Bmatrix} \Lambda^{\xi} \\ \Lambda^{\xi} \end{Bmatrix} \begin{Bmatrix} p \\ q \end{Bmatrix}_{\xi} \\ - k_{\xi+1} \begin{Bmatrix} \Lambda^{\xi+1} \\ \Lambda^{\xi+1} \end{Bmatrix} \begin{Bmatrix} p \\ q \end{Bmatrix}_{\xi+1} = (2\Omega_0 f + f^2) [d]_{\xi} \begin{Bmatrix} p \\ q \end{Bmatrix}_{\xi} \end{aligned} \quad (26)$$

where

$$[k]_{\xi} = \begin{bmatrix} [k^e]^{uu} + [k^{\Omega}]^{uu} & [k^e]^{uv} \\ [k^e]^{uv} & [k^e]^{vv} + [k^{\Omega}]^{vv} - [k^{cv}] \end{bmatrix} \quad (27)$$

and the stiffness matrix $[k^{cv}]$ is introduced by the crack, which is

$$k_{ij}^{cv} = 6 \frac{EI_{xx}}{L^4} (1 - \mu^2) \frac{i_0}{L} (1 - \beta \bar{r}^*) Q(\bar{y}) [\phi_i''(\bar{r}) \phi_j''(\bar{r})]_{\bar{r}=\bar{r}^*} \quad (28)$$

2.3 Equation of motion of the mistuned system

The equation of motion for the entire rotating disk system can be grouped as

$$[M]\{\ddot{X}\} + [K]\{X\} = (2\Omega_0 f + f^2) [D]\{X\} \quad (29)$$

The system stiffness matrix $[K]$ is derived as

$$[K] = \begin{bmatrix} [\alpha]_1 & -k_2[\Lambda] & 0 & \dots & 0 & 0 & -k_1[\Lambda] \\ -k_2[\Lambda] & [\alpha]_2 & -k_3[\Lambda] & \dots & 0 & 0 & 0 \\ 0 & -k_3[\Lambda] & [\alpha]_3 & \dots & 0 & 0 & 0 \\ \dots & \dots & \dots & \dots & \dots & \dots & \dots \\ 0 & 0 & 0 & \dots & [\alpha]_{N-2} & -k_{N-1}[\Lambda] & 0 \\ 0 & 0 & 0 & \dots & -k_{N-1}[\Lambda] & [\alpha]_{N-1} & -k_N[\Lambda] \\ -k_1[\Lambda] & 0 & 0 & \dots & 0 & -k_N[\Lambda] & [\alpha]_N \end{bmatrix} \quad (30)$$

$$\{X\} = \begin{bmatrix} \{p\}_1^T & \{p\}_2^T & \dots & \{p\}_{N-1}^T & \{p\}_N^T \\ \{q\}_1^T & \{q\}_2^T & \dots & \{q\}_{N-1}^T & \{q\}_N^T \end{bmatrix}^T \quad (31)$$

and

$$[\alpha]_s = [k]_s + k_{s+1}[\Lambda] + k_s[\Lambda] \quad \text{for } s = 1, 2, 3, \dots, N \quad (32)$$

Due to the cyclic arrangement of N blades, it leads to

$$\begin{Bmatrix} p \\ q \end{Bmatrix}_{N+1} = \begin{Bmatrix} p \\ q \end{Bmatrix}_1 \quad \text{and} \quad k_1 = k_{N+1} \quad (33)$$

3. ANALYSIS OF THE MISTUNED SYSTEM

Let $[\Psi]$ be the normalized modal matrix of the eigenvalue problem associated with the mistuned system described by Eq. (29). It leads to

$$[\Psi]^T [M] [\Psi] = [I] = \begin{bmatrix} 1 & 0 & 0 & \dots & 0 \\ 0 & 1 & 0 & \dots & 0 \\ \vdots & \vdots & \vdots & \ddots & \vdots \\ 0 & 0 & 0 & \dots & 1 \end{bmatrix} \quad (34)$$

$$[\Psi]^T [K] [\Psi] = [A] = \begin{bmatrix} \omega_1^2 & 0 & 0 & \dots & 0 \\ 0 & \omega_2^2 & 0 & \dots & 0 \\ \vdots & \vdots & \vdots & \ddots & \vdots \\ 0 & 0 & 0 & \dots & \omega_N^2 \end{bmatrix} \quad (35)$$

where $\omega_1^2, \omega_2^2, \dots, \omega_N^2$ are the eigen values of the mistuned system. Using the expansion theorem the response may be described as a superposition of the normal modes in the form

$$\{X\} = [\Psi]\{\eta\} \quad (36)$$

The equation of motion for the mistuned system, i.e., Eq. (29), can be rewritten

$$[I]\{\ddot{\eta}\} + [A]\{\eta\} = -\left(\frac{f}{\Omega_0} + \frac{f^2}{2\Omega_0^2}\right) [D]^* \{\eta\} \quad (37)$$

$$\text{where } [D]^* = -2\Omega_0^2[\Psi]^T[D][\Psi] \quad (38)$$

Let the rotation speed be perturbed by a very small periodic excitation $f(t)$, which can be represented by a Fourier series of harmonic components in the form

$$f(t) = \sum_{j=-Q}^Q F_j e^{i\omega_j t} \quad (39)$$

where ω_j is the harmonic frequency. Introducing Eq. (39) into Eq. (37), the dynamic equation can be rewritten as

$$[I]\{\ddot{\eta}\} + [A]\{\dot{\eta}\} = -\varepsilon \left(\hat{f} + \frac{\varepsilon}{2} \hat{f}^2 \right) [D]^* \{\eta\} \quad (40)$$

with

$$\varepsilon = \frac{|F_M|}{\Omega_0} \quad \text{and} \quad \hat{f}(t) = \frac{f(t)}{|F_M|}$$

where $|F_M|$ is the maximum magnitude of components F_j for $j = 1, 2, \dots, Q$. As assumed, the magnitude of the speed variation $f(t)$ is so small that the ratio ε is less than one. Equation (40) represents a set of N uncoupled differential equations of the type

$$\eta_n + \omega_n^2 \eta_n = -\varepsilon \left(\hat{f} + \frac{\varepsilon}{2} \hat{f}^2 \right) \sum_{m=1}^N d_{nm}^* \eta_m \quad \text{for } n = 1, 2, 3, \dots, N \quad (41)$$

where d_{nm}^* is the element of matrix $[D]^*$. Using the multiple scales method [Nayfeh (1979)], a series of new independent variables are introduced, i.e., $T_\alpha = \varepsilon^\alpha t$ for $(\alpha = 0, 1, 2, \dots)$. It follows that the derivatives with respect to t become

$$\frac{d}{dt} = \frac{dT_0}{dt} \frac{\partial}{\partial T_0} + \frac{dT_1}{dt} \frac{\partial}{\partial T_1} + \dots = D_0 + \varepsilon D_1 + \dots \quad (42)$$

$$\frac{d^2}{dt^2} = D_0^2 + 2\varepsilon D_0 D_1 + \varepsilon^2 (D_1^2 + 2D_0 D_2) + \dots \quad (43)$$

Consider that the solution for equation (40) can be represented by an expansion form

$$\eta_n(t; \varepsilon) = \eta_{n0}(T_0, T_1, T_2, \dots) + \varepsilon^1 \eta_{n1}(T_0, T_1, T_2, \dots) + \varepsilon^2 \eta_{n2}(T_0, T_1, T_2, \dots) + \dots \quad (44)$$

Substitute Eqs (42), (43) and (44) into Eq. (41), and equating the coefficients of $\varepsilon^0, \varepsilon^1, \varepsilon^2, \dots$. This yields

$$\text{order } \varepsilon^0 \quad D_0^2 \eta_{n0} + \omega_n^2 \eta_{n0} = 0 \quad (45a)$$

$$\text{order } \varepsilon^1 \quad D_0^2 \eta_{n1} + \omega_n^2 \eta_{n1} = -2D_0 D_1 \eta_{n0} - \hat{f} \sum_{r=1}^N d_{nr}^* \eta_{r0} \quad (45b)$$

The general solution for equation (45a) can be written in the form

$$\eta_{n0} = A_n(T_1, T_2) \exp(i\omega_n T_0) + c.c. \quad (46)$$

where $A_n(T_1, T_2)$ is an unknown complex function, and *c.c.* denotes the corresponding complex conjugate of the preceding term. For simplicity, the periodic speed perturbation is assumed

$$\hat{f} = \sum_{j=1}^Q \hat{F}_j e^{i\omega_j t} + c.c. \quad (47)$$

Substituting the general solution (46) into equation (45b), it leads to

$$D_0^2 \eta_{n1} + \omega_n^2 \eta_{n1} = -2i\omega_n (D_1 A_n) e^{i\omega_n T_0} - \sum_{j=1}^Q \hat{F}_j \sum_{r=1}^N d_{nr}^* \left\{ A_r e^{i[\omega_r + \omega_j] T_0} + \bar{A}_r e^{i[\omega_r - \omega_j] T_0} \right\} + c.c. \quad (48)$$

where \bar{A}_r denotes the complex conjugate of A_r . The complex coefficient A_n is to be determined in such a way as to eliminate the troublesome terms from η_{n1} . This choice depends upon the resonant combinations of the frequencies; four different cases are considered herein [Nayfeh and Mook (1979), Young (1991)].

(i) When ω_j is away from frequencies $(\omega_p \pm \omega_q)$

In this case, a particular solution for η_{n1} in Eq. (48) can be solved by eliminating the term $-2i\omega_n (D_1 A_n) e^{i\omega_n T_0}$.

$$\eta_{n1} = \sum_{j=1}^Q \hat{F}_j \sum_{r=1}^N d_{nr}^* A_r \left\{ \frac{\exp[i(\omega_r + \omega_j) T_0]}{(\omega_r + \omega_j)^2 - \omega_n^2} + \frac{\exp[i(\omega_j - \omega_r) T_0]}{(\omega_j - \omega_r)^2 - \omega_n^2} \right\} + c.c. \quad (49)$$

It reveals that the mistuned system keeps stable in this case.

(ii) When $\omega_j \rightarrow (\omega_p + \omega_q)$

In this so called combination resonance of the summed type case, the character of the solution is modified drastically and the transition curves between the stable and unstable zone is given by

$$\omega_j = \omega_p + \omega_q \pm \varepsilon \sqrt{\sum_{j=1}^Q \hat{F}_j^2 \Lambda_{pq}} \quad (50)$$

where $\Lambda_{pq} = (d_{pq}^* d_{qp}^*) / (\omega_p \omega_q)$.

(iii) When $\omega_j \rightarrow (\omega_p - \omega_q)$

The transition curves of combination resonance of the different type can be solved as

$$\omega_j = \omega_p - \omega_q \pm \varepsilon \sqrt{-\sum_{j=1}^Q \hat{F}_j^2 \Lambda_{pq}} \quad (51)$$

However, this case may occur only as d_{pq}^* and d_{qp}^* have different signs.

(iv) When $\omega_j \rightarrow (\omega_p + \omega_q)$ and $(\omega_q + \omega_s)$

The transition curves have to be amended, if the perturbation frequency ω_j nears the combination resonance of the summed type $\omega_p + \omega_q$ and nears simultaneously $\omega_q + \omega_s$. In this case, after tedious derivation, the equation can be solved for determining the stability and instability of the system. It is given by

$$\lambda^3 + (\sigma_1 + \sigma_2) \lambda^2 + \left(\sigma_1 \sigma_2 + \frac{1}{4} (\Lambda_{qs} + \Lambda_{pq}) \sum_{j=1}^Q \hat{F}_j^2 \right) \lambda$$

$$+\frac{1}{4}(\sigma_1 \Lambda_{qs} + \sigma_2 \Lambda_{pq}) \sum_{j=1}^Q \hat{F}_j^2 = 0 \quad (52)$$

where

$$\sigma_1 = \frac{\omega_j - \omega_p - \omega_q}{\varepsilon} \quad \text{and} \quad \sigma_2 = \frac{\omega_j - \omega_p - \omega_s}{\varepsilon}$$

Equation (52) is a cubic equation for λ and has closed-form solutions. The transition curves can be determined using the value of ω_j for which λ has two real roots.

4. NUMERICAL RESULTS AND DISCUSSION

An assembly of 46 pretwisted taper beams attached to a rigid hub was used to approximate the turbo-disk as shown in Figure 1(a). A shroud spring k_s was attached at the tip of each blade. The blades were specified using the following non-dimensional parameters: $(R_h/L) = 0.2$, $(b_o/L) = 0.1$, $(t_o/L) = 0.02$, $\alpha = \beta = 0.25$, $\theta = 45^\circ$ and $\bar{r}^* = 0$. For convenience, a number of non-dimensional parameters, i.e., $\bar{\omega} = \omega/\omega_0$, $\bar{\omega}_n = \omega_n/\omega_0$, $\bar{\Omega}_0 = \Omega_0/\omega_0$ and $\bar{k}_s = (12k_s L^3)/Eb_o t_o^3$, were also used. The frequency ω_n is the natural frequency of the mistuned system, and ω_0 is a reference frequency that is defined herein as

$$\omega_0 = 0.01 \sqrt{\frac{E}{\rho L^2}}. \quad \text{As a crack propagates on a blade, it may}$$

introduce the so called 'modal localization phenomenon' in the entire mistuned system. The amplitudes of individual defective blades may in turn be excited seriously. The localized vibrations further increase the amplitudes and stresses locally. In this example, the localization stability of a cracked blade-disk system was investigated. For simplicity, a single crack at the root of the 23rd blade was assumed. The effects of crack depth α , shroud stiffness k_s and rotational speed Ω_0 of the blade on the stability were studied.

Before considering the dynamic stability of a cracked blade-disk system, it is appropriate first to illustrate the characteristics of the cracked system. To this end, one identifies the modal localization of this cracked system. Figure 2 shows the corresponding blade tip displacement patterns of the cracked blade-disk system in the rotational plane and the out-off plane at the localization frequency, i.e., the lowest natural frequency. An obvious modal localization phenomenon is observed for this mistuned system. The corresponding frequency response at the tip of the cracked 23rd blade is displayed in Fig. 3. It indicates that a group of peak of responses are observed near the localization frequency. To determine the stability of a rotating blade-disk, a simplified harmonic perturbation speed as $f(t) = 2 \cos \omega t$ is assumed to be imposed on the steady speed Ω_0 . Figure 4(a) displays the stable and the unstable bands according to the stability analysis of a cracked blade-disk. The first unstable band is grouped from a series of unstable zones near the resonance frequencies $(2\bar{\omega}_1 \sim 2\bar{\omega}_{46})$, as shown in Fig. 4(b). As noted in Fig. 3, the modal localization phenomenon will introduce a group of peaks of response near the localization frequency. Resonant

frequencies are always distributed in a cluster for a locally defected periodic system [Wei and Pierre (1988a, 1998b), Bendiksen (1987)]. Thus, the range of this unstable zone is dependent upon the spread of the resonant frequencies from $2\bar{\omega}_1$ to $2\bar{\omega}_{46}$. These unstable zones related to resonant frequencies $(2\bar{\omega}_1, 2\bar{\omega}_2, \dots, 2\bar{\omega}_{46})$ are distributed so close that they could hardly be separated. According to the stability analysis of this cracked blade-disk, some small stable regions are found near the resonant frequencies $(2\bar{\omega}_1, 2\bar{\omega}_2, 2\bar{\omega}_3)$ as shown in Figure 4(b). However, these very small stable regions have a negligible impact upon the system.

Figures 5(a) and 5(b) demonstrate the important role of the crack depth upon the variations in the transition curves. Results indicate that the unstable zone near $2\bar{\omega}_1$ will be shifted left if the depth of the crack in the 23rd blade is increased from $\bar{\gamma} = 0.01$ to $\bar{\gamma} = 0.1$. As noted [Kuang *et al* (1998)], increasing the crack depth may enhance the modal localization and shift the localization frequency $2\bar{\omega}_1$ down. This localization frequency shift, from $2\bar{\omega}_1 = 4.669$ to $2\bar{\omega}_1 = 4.656$, will enlarge the unstable band as shown in Figure 5(b). The effect of the rotational speed $\bar{\Omega}_0$ on the variations in the unstable bands is illustrated in Figures 6(a) and 6(b). Because additional stiffness will be introduced into the blades as the blade speed is increased, the modal frequency is increased. It can be observed that the first unstable band is enlarged and shifted toward a higher frequency region. As noted by a number of articles, the degree of localization depends significantly upon the magnitude of the disorder and the modal coupling effect. The modal coupling effect in this periodic blade-system is dominated by the spring stiffness constant \bar{k}_s . For a mistuned system, that strong localization may occur in a weakly coupled system [Pierre (1990)]. The effect of shroud stiffness on the stability is also shown in Figure 7(a) and 7(b). This apparent enlargement in the unstable band, as the coupling stiffness is increased from $\bar{k}_s = 0.02$ to $\bar{k}_s = 0.10$, is believed to be caused by a change in the modal localization pattern. The frequency band $(2\bar{\omega}_1 \sim 2\bar{\omega}_{46})$ would well as the coupling stiffness is increased.

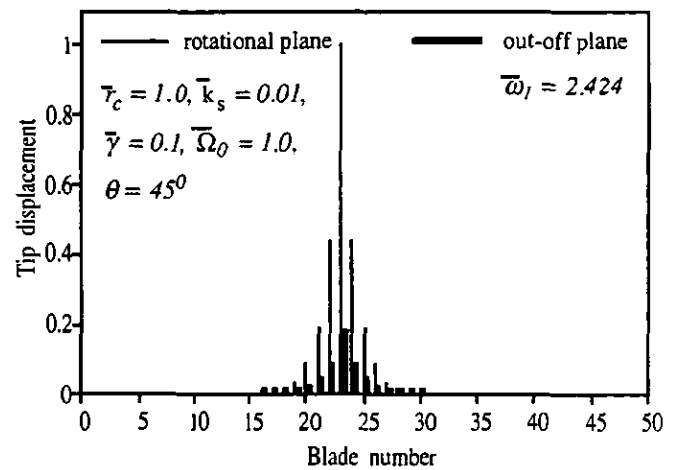


Figure 2 Tip displacement patterns of a cracked blade-disk system

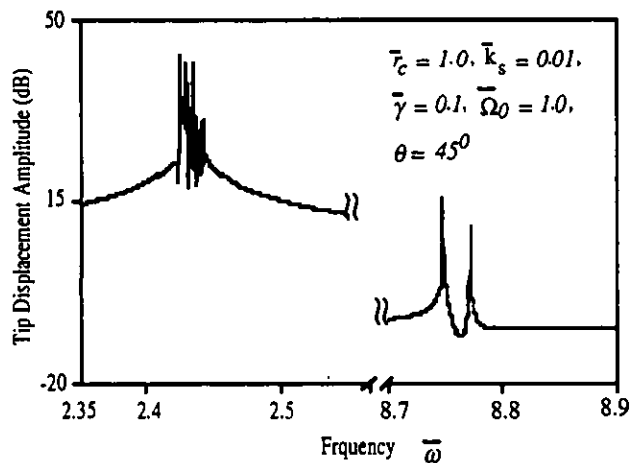
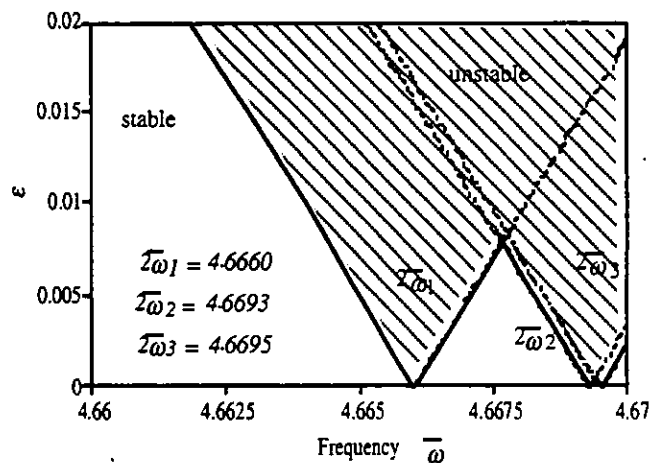
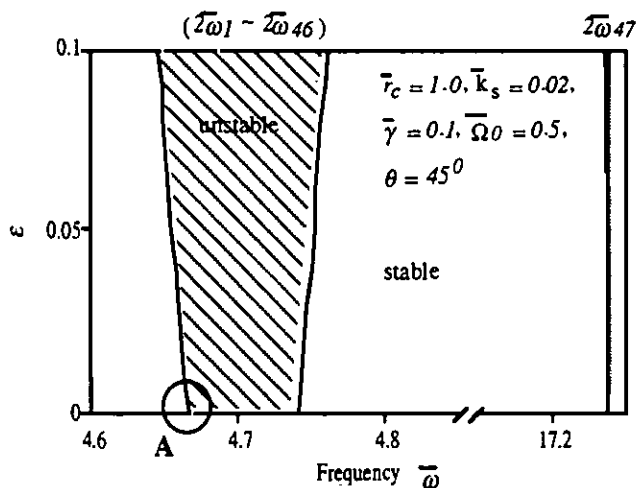


Figure 3 Tip frequency response at the tip of the 23rd blade

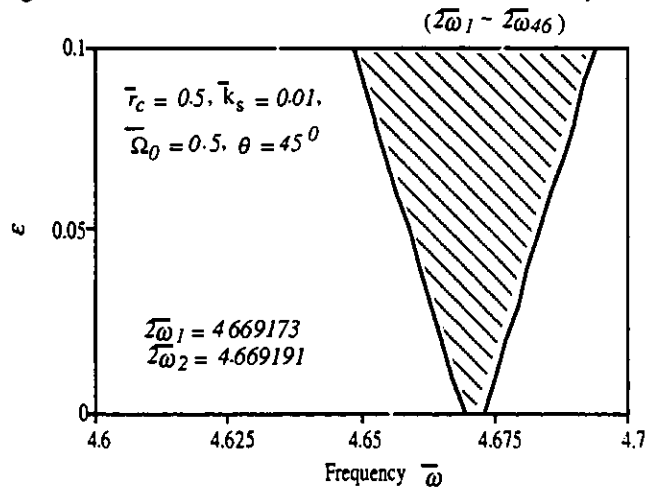


(b) the detail for zone A

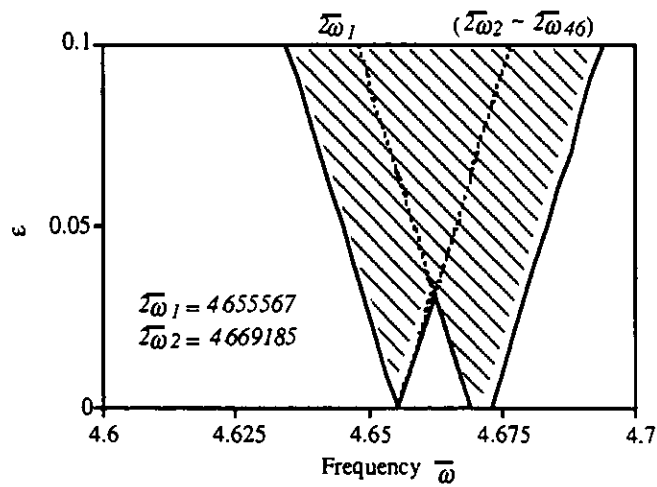
Figure 4 Transition curves for the cracked blade-disk system



(a) the regions of instability



(a) crack $\bar{\gamma} = 0.01$



(b) crack $\bar{\gamma} = 0.1$

Figure 5 The variations in the transition curves for different

5. CONCLUSIONS

Blade crack has been shown to be sensitive to the stability of a rotating blade disk. The modal localization phenomenon caused by the local defect may enhance the unstable band significantly. The major conclusions that can be drawn from the above analysis and the preceding discussion are

- (1) According to the proposed stability analysis, a series of closely located unstable zones are introduced by the modal localization effect. These instability zones may swell as the inter-blade coupling stiffness is increased.
- (2) The depth of a crack is one of the most important parameters for stability in a rotating mistuned blade-disk system. Results indicate that the first unstable band might be enlarged as the depth of the crack increases.

- (3) It is clear that the rotational speed of a mistuned disk has a significant influence on the instability. It will shift the unstable band towards a higher frequency region.

6. REFERENCE

Afolabi, D., 1985, "The Eigenvalue Spectrum of Mistuned Bladed Disk," *Vibrations of Blades and Bladed Disk Assemblies, Proceedings of the Tenth Biennial Conference on Mechanical Vibration and Noise*, Cincinnati, Ohio.

Anderson G. L., 1975, "On the Extensional and Flexural Vibrations of Rotating Bar," *International Journal of Nonlinear Mechanics*, Vol. 10, pp. 223-236.

Basu, P. and Griffin, J. H., 1985, "The Effect of Limiting Aerodynamic and Structural Coupling in Models of Mistuned Blade Disk Vibration," *ASME Journal of Vibration, Acoustics, Stress, and Reliability in Design*, Vol. 108, pp. 132-139.

Bendiksen, O. O., 1984, "Flutter of Mistuned Turbo

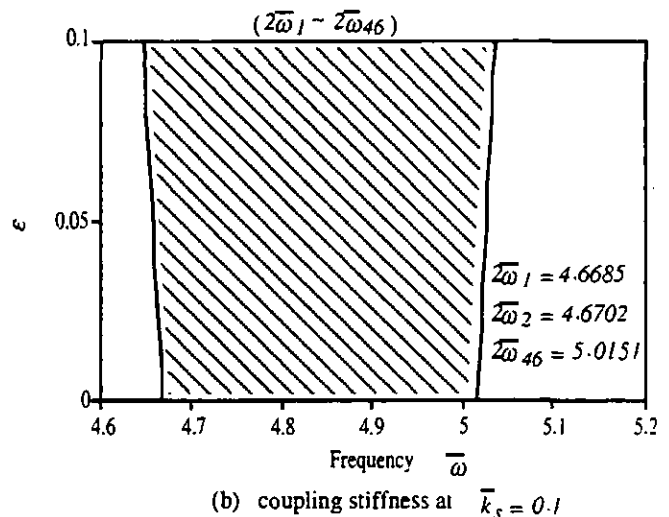
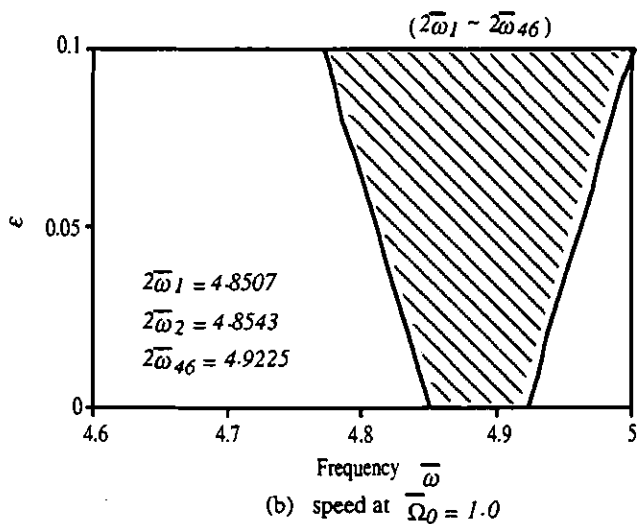
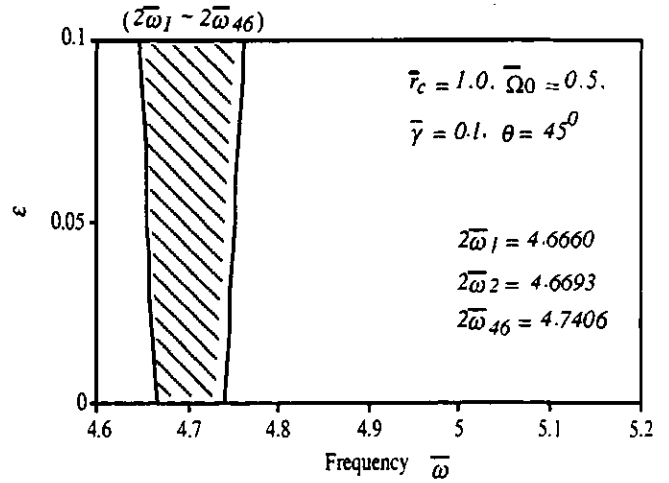
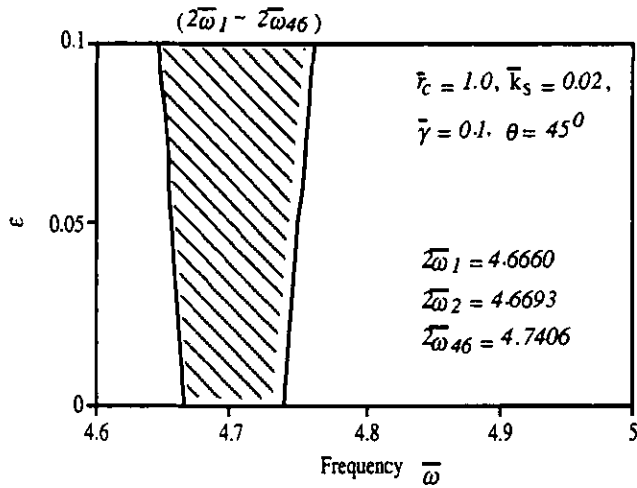


Figure 6 The variations in the transition curves for different rotating speeds

Figure 7 The variations in transition curves for different coupling stiffness

machinery Rotors," *ASME Journal of Engineering for Gas Turbines and Power*, Vol. 106, pp. 25-23

Bendiksen, O. O., 1987, "Modal localization phenomena in Large Space Structures," *AIAA Journal*, Vol. 25, pp. 1241-1248.

Bernstein, H. L. and Alien, J. M., 1992, "Analysis of Cracked Gas Turbine Blades," *ASME Journal of Engineering for Gas Turbines and Power*, Vol. 114, pp. 293-301.

Broek D., 1986, *Elementary Engineering Fracture mechanics*, Martinus Nijhoff Publishers.

Chen L. and Chen C., 1988, "Vibration and Stability of Cracked Thick Rotating Blade," *Computers & Structures*, Vol. 28, No. 1, pp. 67-74.

Cottney, D. J. and Ewins, D. J., 1974, "Towards the Efficient Vibration Analysis of Shrouded Bladed Disk Assemblies," *ASME Journal of Engineering for Industry*, Vol. 96B, pp. 1054-1059.

Dimarogonas, A. D., and Paipetis, S. A., 1983, *Analytical Methods in Rotor Dynamics*, Applied Science Publishers, New York.

Hodges, C. H., 1982, "Confinement of Vibration by Structural Irregularity," *Journal of Sound and Vibration*, Vol. 82, No. 3, pp. 411-424.

Hsu C. S., 1961, "On a Restricted Class of Coupled Hill's Equations and Some Applications," *ASME Journal of Applied Mechanics*, pp. 551-557.

Grabowski B., 1980, "The Vibrational Behavior of a Turbine Rotor Containing a Transverse Crack," *ASME Journal of Mechanic Design*, Vol. 102, pp. 140-146.

Kaneko, Y., Mase, M., Fujita, K., and Nagashima, T., 1994, "Vibration Response Analysis of Mistuned Bladed Disk," *JSME International Journal Series C*, Vol. 37, No. 1, pp. 33-40.

Krawczuk, M. and Ostachowicz, W. M., 1993, "Transverse Natural Vibrations of a Cracked Beam Loaded with a Constant Axial Force," *ASME Journal of Vibration and Acoustics*, Vol. 115, pp. 524-528.

Kuang, J. H. and Huang, B. W., 1997, "Coriolis Effect on Modal localization in a Rotating Bladed Disk," *Proc. of DETC'97*, ASME, *Design Engineering Technical Conference*, September 14-17, Sacramento, California, Paper No. DETC97/VIB-4065.

Kuang, J. H. and Huang, B. W., 1998, "Modal localization of a Cracked Bladed Disk," *Proc. of Turbo Expo'98*, The 43rd ASME Gas Turbine and Aeroengine Congress, June 2-5, Stockholm, Sweden, Paper No. 98-GT-105.

Lee, H. P., 1995, "Effects of Axial Base Excitations on The Dynamic Stability of Spinning Pretwisted Cantilever Beams," *Journal of Sound and Vibration*, Vol. 185, No. 2, pp. 265-278.

Liao C. L. and Huang B. W., 1995, "Parametric Resonance of a spinning Pretwisted Beam with Time-Dependent Spinning Rate," *Journal of Sound and Vibration*, Vol. 180, No. 1, pp. 47-65.

Nayfeh A. H., and Mook D. T., 1979, *Nonlinear Oscillation*, New York: John Wiley.

Orgun C. O. and Tongue, B. H., 1994, "Modal localization in Coupled Circular Plates," *ASME Journal of Vibration and Acoustics*, Vol. 116, pp. 286-294

Rao, J. S., 1972, "Flexural Vibration of Pretwisted tapered Cantilever Blades," *ASME Journal of Engineering for Industry*, Vol. 94, No. 1, pp. 343-346.

Rao, J. S., 1977, "Vibration of Rotating, Pretwisted and Tapered Blades," *Mechanism and Machine Theory*, Vol. 12, pp. 331-337.

Rizos, P. F., Aspragathos, N. and Dimarogonas, A. D., 1990, "Identification of Crack Location and Magnitude in a Cantilever Beam from the Vibration Mode," *Journal of Sound and Vibration*, Vol. 138, pp. 381-388.

Tada H., Paris P. and Irwin G., 1973, *The Stress Analysis of Crack Handbook*, Hellertown, Pennsylvania : Del Research Corporation.

Walls, D. P., deLaneuville, R. E. and Cunningham, S. E., 1997, "Damage Tolerance Based Life Prediction in Gas Turbine Engine Blades under Vibratory High Cycle Fatigue," *ASME Journal of Engineering for Gas Turbines and Power*, Vol. 119, pp. 143-146.

Wei, S. T. and Pierre, C., 1988, "Localization Phenomena in Mistuned Assemblies with Cyclic Symmetry part I: Free Vibrations," *ASME Journal of Vibration, Acoustics, Stress, and Reliability in Design*, Vol. 110, pp. 429-438.

Wei, S. T. and Pierre, C., 1988, "Localization Phenomena in Mistuned Assemblies with Cyclic Symmetry part II :Forced Vibrations," *ASME Journal of Vibration, Acoustics, Stress, and Reliability in Design*, Vol. 110, pp. 439-449.

Young, T. H., 1991, "Dynamic Response of A Pretwisted, Tapered Beam with Non-constant Rotating Speed," *Journal of Sound and Vibration*, Vol. 150, No. 3, pp. 435-446.

Acknowledgments- The authors would like to acknowledge the support of the National Science Council, R. O. C., through grant no. NSC87-2212-E-110-004.